Combined Triplex/Duplex Invasion of Double-Stranded DNA by "Tail-Clamp" Peptide Nucleic Acid†

Thomas Bentin, H. Jakob Larsen,‡ and Peter E. Nielsen*

Center for Biomolecular Recognition, IMBG, Department B, The Panum Institute, University of Copenhagen, Blegdamsvej 3c, 2200 Copenhagen N, Denmark

Received July 8, 2003; Revised Manuscript Received September 22, 2003

ABSTRACT: "Tail-clamp" PNAs composed of a short (hexamer) homopyrimidine triplex forming domain and a (decamer) mixed sequence duplex forming extension have been designed. Tail-clamp PNAs display significantly increased binding to single-stranded DNA compared with PNAs lacking a duplex-forming extension as determined by T_m measurements. Binding to double-stranded (ds) DNA occurred by combined triplex and duplex invasion as analyzed by permanganate probing. Furthermore, C_{50} measurements revealed that tail-clamp PNAs consistently bound the dsDNA target more efficiently, and kinetics experiments revealed that this was due to a dramatically reduced dissociation rate of such complexes. Increasing the PNA net charge also increased binding efficiency, but unexpectedly, this increase was much more pronounced for tailless-clamp PNAs than for tail-clamp PNAs. Finally, shortening the tail-clamp PNA triplex invasion moiety to five residues was feasible, but four bases were not sufficient to yield detectable dsDNA binding. The results validate the tail-clamp PNA concept and expand the applications of the P-loop technology.

Versatile, efficient, and sequence-specific targeting of double-stranded (ds) DNA by designed synthetic molecules is a major contemporary objective in DNA molecular biology research. Sequence-specific targeting of dsDNA by the DNA mimic peptide nucleic acid (PNA) can occur via several distinct mechanisms depending on the DNA target and the PNA sequence. The most stable complexes are formed with homopyrimidine PNAs targeting homopurine DNA via triplex invasion and P-loop formation (Figures 1a and 2a) (*1*−*5*). Complexes of approaching stability can be obtained using a pair of pseudocomplementary PNA oligomers that bind by double-duplex invasion (Figures 1b and 2b) (*6*−*8*). Under certain conditions simple duplex invasion complexes can form (Figure 1c). These are much less stable than comparably sized triplex or double-duplex invasion complexes and have so far only been observed with very purine rich PNA oligomers (*9*) or with cationic peptide−PNA conjugates (*10*) binding to DNA targets under negative superhelical stress.

As the formation of P-loop complexes is of great interest for both gene targeting (*11*−*14*) and a variety of diagnostic and molecular biology applications (*15*−*19*), we decided to explore the binding properties of "tail-clamp" PNA oligomers comprising a triplex as well as a duplex-forming domain. Ideally, such PNAs would bind their complementary target in double-stranded DNA by a combined triplex/duplex invasion mechanism (Figure 1d). Provided that the duplex domain would contribute sufficiently to the binding energy, this binding mode would only require a relatively short homopurine stretch in the target, and therefore the target sequence constraints for P-loop formation would be greatly relaxed.

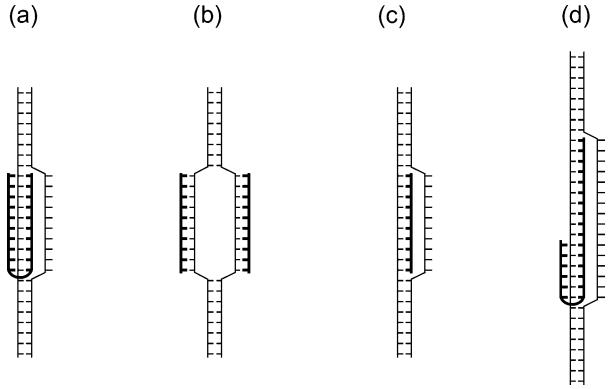

FIGURE 1: Structure of helix invasion complexes. (a) Triplex invasion complex: structure of homopyrimidine bis-PNA bound to a dsDNA target. The two PNA strands clamp onto the complementary DNA strand leaving the noncomplementary DNA strand displaced as a loop. (b) Double duplex invasion complex: pseudocomplementary- (pc-) PNAs bound to a cognate sequence target in dsDNA. Each pc-PNA strand binds by Watson−Crick base pairing, thus occupying both target DNA strands. (c) Duplex invasion complex: one PNA strand invades the DNA helix forming Watson−Crick hydrogen bonds, thus leaving the noncomplementary DNA strand displaced. (d) Principle of tail-clamp PNA invasion complex. The homopyrimidine clamp domain binds by combined Watson−Crick and Hoogsteen hydrogen bonds while the duplex extension employs Watson−Crick interactions only.

We have now synthesized a series of such tail-clamp PNA oligomers containing a decamer duplex domain and varying size (4−6 bases) triplex domains and measured their binding

† This work was supported by the Lundbeck Foundation, EU Contract QLK-3-CT-2000-00634, and by the Danish Research Agency.

* Corresponding author. E-mail: pen@imbg.ku.dk.

‡ Present address: Department of Forensic Genetics, Institute of Forensic Medicine, University of Copenhagen, Frederik V's Vej 11, 2100 Copenhagen Ø, Denmark.

10.1021/bi0351918 CCC: $25.00
Published on Web 11/05/2003

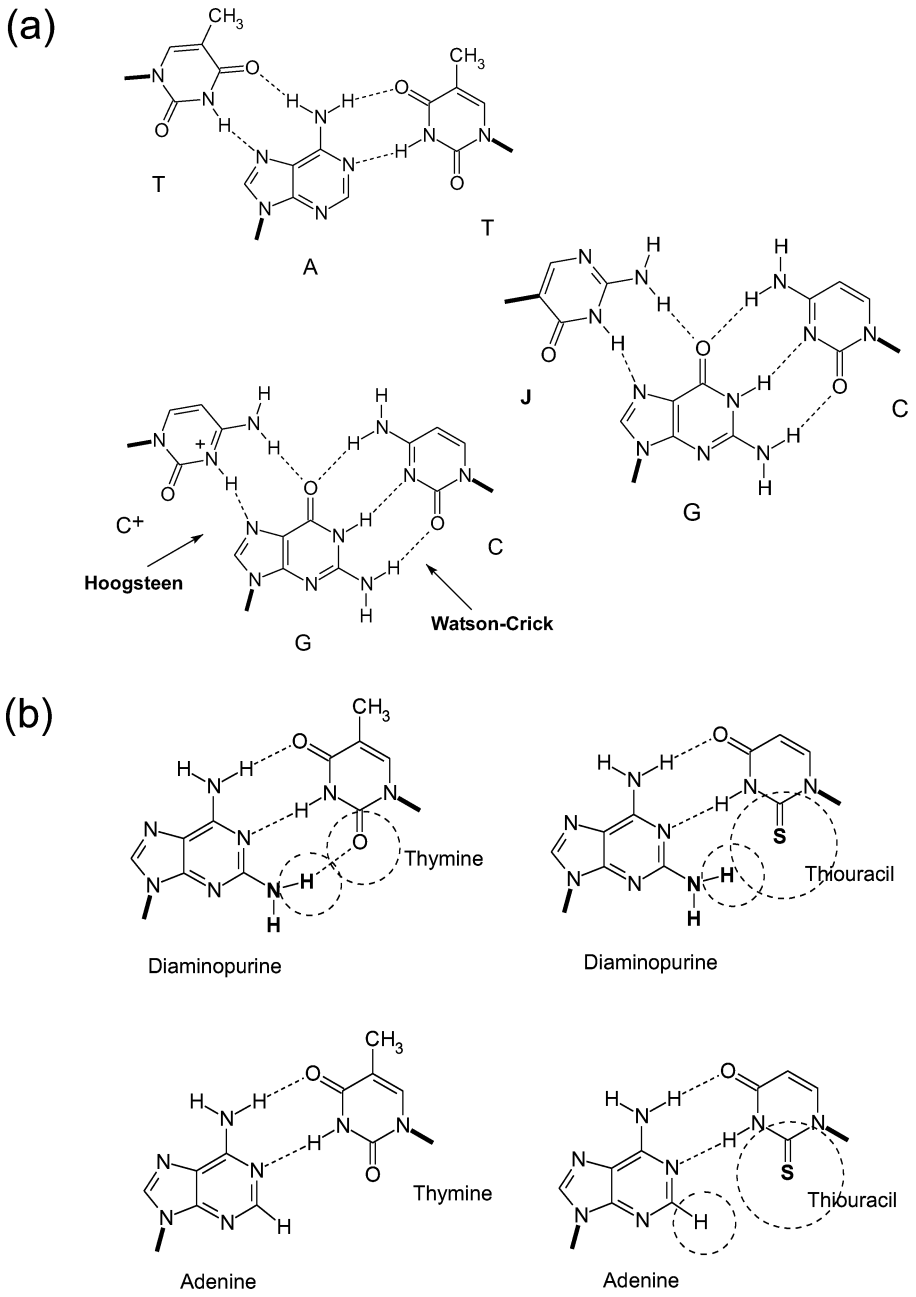

FIGURE 2: Hydrogen bonds in strand invasion complexes. (a) Base triads in the triplex invasion complex involving Hoogsteen and Watson−Crick hydrogen bonds as indicated. J = pseudoisocytosine. (b) Principle of base interactions in double-duplex invasion complexes. pc-PNAs have diaminopurine (D) and thiouracil (U^s) substituted for adenine and thymidine, respectively. The atomic radii of the D exocyclic amino group and the 2-thio group of U^s inhibit D−U^s hydrogen bonding, thereby reducing self-annealing of pc-PNAs. In contrast, D−T and A−U^s hybridization is not subject to such constraints, which facilitates hybridization to complementary DNA targets.

efficiency to a target in a double-stranded DNA fragment by permanganate probing of P-loop formation. We have also varied the charge (1+ to 5+) of such tail-clamp PNAs.

EXPERIMENTAL PROCEDURES

PNA Molecules. The PNA sequences used in this study are listed in Table 1. The PNAs were synthesized and characterized as described previously (*20*). PNA stocks were dissolved at 50 OD_{260}/mL in doubly distilled H_2O and stored at −20 °C. Low-stick tubes from Soerensen Biosciences (catalog no. 11720) were used throughout. "J" denotes the synthetic nucleobase pseudoisocytosine (*21*). PNA concentrations were determined using the following extinction coefficients: ϵ_{260} = 8800 M^{-1} cm^{-1} (T), 15 500 M^{-1} cm^{-1} (A), 11 700 M^{-1} cm^{-1} (G), 7300 M^{-1} cm^{-1} (C), and 3000 M^{-1} cm^{-1} (J).

DNA Construct. Two complementary oligonucleotides (5′-dTCGACTTTTTG-3′ and 5′-dTCGACAAAAAG-3′) were annealed and inserted into the *Sal*I site of pUC19 by standard cloning methods (*22*). The resulting construct was verified by sequencing, digested with *Pvu*II and *Hin*dIII, and 10 μg of DNA was end-labeled using [α-^{32}P]dATP and the Klenow fragment of *Escherichia coli* DNA polymerase I as recommended by the manufacturer (Gibco BRL). The relevant DNA fragment (155 bp) was isolated using nondenaturing 5% polyacrylamide gel electrophoresis.

Table 1: T_m and C_{50} Values for Tail-Clamp PNA Hybridization to ssDNA and dsDNA[a]

PNA oligomer	Tm*	Tm**	C_{50}
PNA355 (+1) H-TTTTTJ / H_2N-CGTCCAGCTGTTTTTC	84 (74)	53	2.5 ± 0.2
PNA472 (+1) H-TTTTTJ / H_2N-TTTTTC	44	42	>250 (#)
PNA350 (+2) H-TTTTTC / H_2N-CGTCCAGCTGTTTTTC	83 (73)	49	0.4 ± 0.1
PNA2305 (+2) H-TTTTTC / H_2N-TTTTTC	43	37	39 ± 13 (#)
PNA602 (+3) H-TTTTTC / H_2N-Lys-CGTCCAGCTGTTTTTC	83 (73)	50	0.19 ± 0.09
PNA2306 (+3) H-Lys-TTTTTC / H_2N-TTTTTC	45	38	6.5 ± 1.7 (#)
PNA2307 (+4) H-Lys_2-TTTTTC / H_2N-TTTTTC	47	39	0.9 ± 0.6 (#)
PNA603 (+5) H-Lys_2-TTTTTC / H_2N-Lys-CGTCCAGCTGTTTTTC	85 (74)	51	0.09 ± 0.04
PNA601 (+5) H-Lys_2-TTTTTC / H_2N-Lys-TTTTTC	49	42	1.4 ± 0.5 (#)
PNA648 (+5) H-Lys_2-TTTT / H_2N-Lys-CGTCCAGCTGTTTT	77 (63)	40	Nd
PNA649 (+5) H-Lys_2-TTTTT / H_2N-Lys-CGTCCAGCTGTTTTT	83 (70)	50	0.12 ± 0.04
PNA231 (+3) H-TTTTTC / H_2N-Lys-CCAGCAGCTGTTTTTC	78 (67)	52	0.8 ± 0.2
PNA497 (+1) H_2N-CGTCCAGCTG-H	66 (~50[a])	Nd	Nd
PNA357 (+1) H-TTTTTC / H_2N-CGTCCAGCTGTTTTTC	76 (63)	47	4 ± 0.1

[a] The table shows the structure, net charge, thermal melting temperature (T_m), and C_{50} values (μM) of the PNAs employed. T_m is given in degrees Celcius. T_m*: T_m measured for hybridization to the full-length single-stranded target 5′-dGCAGGTCGACAAAAAG-3′ (oligo Me551). The T_m values for hybridization to the singly mismatched target 5′-dGCAGGTCCACAAAAAG-3′ (oligo Me551-1mis; the mismatched position is underlined) are given in parentheses. T_m**: T_m for binding to the hexamer single-stranded target 5′-dAAAAAG-3′ (oligo Me81). (a) T_m based on broad transition. C_{50} values are expressed ± standard error of the mean using two to five experiment repetitions. The (#) label indicates C_{50} values that are shown (PNA601) or expected (PNA472, PNA2305, PNA2306, and PNA2307) to represent true equilibrium constants. The C_{50} for PNA472, which bound very poorly, was estimated by extrapolation. Nd: not determined. The bis-PNA linkers aminohexanoic acid (PNA350, PNA2305, PNA602, PNA2306, PNA2307, PNA603, PNA601, PNA648, PNA649, and PNA231) and 8-amino-2,6-dioxaoctanoic acid (PNA355, PNA472, and PNA357) were used as described (*21*, *25*). PNA497 does not contain a linker moiety.

T_m Determinations. The melting temperature (T_m) at which 50% of the molecules are hybridized was determined by recording the absorbance at 260 nm as a function of temperature using 4 μM complementary strands in 100 mM NaCl, 10 mM sodium phosphate, and 0.1 mM EDTA, pH 7, as described elsewhere (*23*).

Triplex/Duplex Invasion and $KMnO_4$ Probing. End-labeled DNA at a final estimated concentration of 1−2 nM was incubated with the desired amount of PNA in a total volume of 100 μL of sodium phosphate, pH 6.5, for 2 h at room temperature followed by oxidation with 5 μL of 20 mM $KMnO_4$ for 15 s. The reactions were stopped by adding 50 μL of 1 M β-mercaptoethanol and 1.5 M sodium acetate, pH 9. The oxidized DNA was precipitated with ethanol, treated with 100 μL of 10% (v/v) piperidine (20 min at 90 °C), and lyophilized. The samples were dissolved in forma-

mide loading buffer, resolved on 10% polyacrylamide denaturing TBE-buffered gels, and visualized by autoradiography and phosphorimaging. For kinetic measurements, a mastermix containing material sufficient for the entire experiment was set up. At the desired length of incubation aliquots were removed and probed with permanganate. Off-rates were measured by adding a molar surplus of oligonucleotide complementary to the PNA. Control experiments showed that this efficiently quenched free PNA oligomers as no PNA−dsDNA association was detected if the quench oligonucleotide was added prior to PNA.

All quantitative analyses were done by phosphorimaging of sequencing gels using a Molecular Dynamics phosphorimager and ImageQuant software. C_{50} values were determined by plotting the permanganate-probing signal, which reflects the amount of PNA/dsDNA invasion complex (PD complex) formed, as a function of PNA concentration followed by nonlinear regression analysis using Prism software. To determine the permanganate-probing signal corresponding to 100% PNA binding, the signal plateau was estimated, whenever possible, by including two consecutive "high" PNA concentrations that gave roughly the same signal intensity. When binding was incomplete (PNA472 and PNA2305), the signal was taken relative to the correspondingly charged tail-clamp PNAs. Figure error bars indicate the standard error of the mean using two to five experiment repetitions.

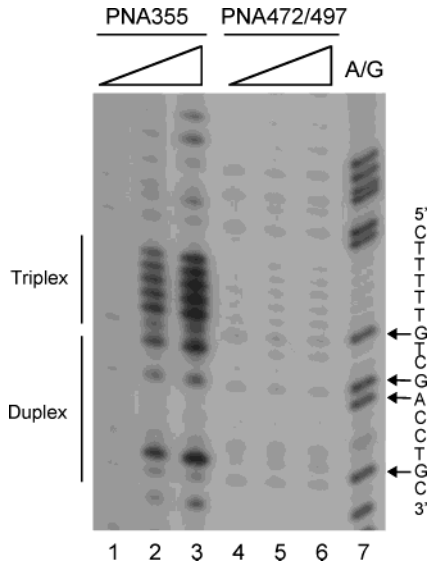

FIGURE 3: Effect of the duplex-forming tail in cis versus in trans. The autoradiograph shows strand invasion by tail-clamp PNA (PNA355, 1+) and homopyrimidine bis-PNA (PNA472, 1+) to which a duplex-forming tail (PNA497, 1+) is added in trans as determined by permanganate probing. Note that the PNA472/PNA497 combination does not bind even though the tail provides an extra charge, making the final charge 2+ for this combination. The following PNA concentrations were used: 0.3 μM (lanes 1 and 5), 0.8 μM (lanes 2 and 6), and 2.5 μM (lanes 3 and 7). A/G = sequence marker.

RESULTS

Design of PNA Oligomers. It has been found that bis-PNA clamps as short as seven to eight nucleobases bind stably to their target (*5*). We therefore based our tail-clamp PNA design on a hexameric clamp domain, which is not expected to exhibit efficient binding to a dsDNA target. Thus any additional binding energy provided by a duplex domain should be readily detectable. For the duplex domain we chose a decamer as this would result in a PNA recognizing 16 bases, which is statistically unique in the sequence of the human genome.

Tail-Clamp PNA Binding to Single-Stranded DNA. To characterize the binding properties of tail-clamp PNAs, we first determined the thermal stability (T_m) of the PNA complexes with two different oligodeoxyribonucleotides (Table 1). One of the oligonucleotides constitutes a hexadecamer full-length target to which the tail-clamp PNAs may bind in a combined duplex/triplex mode. The other oligonucleotide is a target for the PNA triplex forming region only.

Not surprisingly, tail-clamp PNA hybridization to the full-length target exhibits dramatically increased thermal stability (T_m 76−85 °C) as compared with the bis-PNAs lacking a duplex-forming extension (T_m 43−49 °C) (Table 1). This is expected because the duplex-forming tail in isolation (PNA497) hybridizes to its cognate target with a substantial T_m (66 °C).

The effects of introducing a single G → C mismatch in the DNA target duplex region proximal to the homopurine PNA clamp target revealed a marked decrease of resulting thermal melting temperatures ranging from 10 to 14 °C (Table 1). When mismatches were introduced distally in the duplex PNA tail (compare PNA231 and PNA602 in Table 1), the decrease in T_m was only 5 °C even with three consecutive mismatches. This indicates that the PNA duplex forming tail does indeed confer specificity to the recognition and, as could be expected, in a position-dependent manner.

Interestingly, tail-clamp PNA binding to the truncated hexamer DNA target was superior by 9−12 °C as compared with the homopyrimidine bis-PNAs. This effect is ascribed to the additional stacking interactions within the duplex extension.

PNAs having only four or five bases instead of six bases in the triplex-forming region were used to investigate the importance of the triplex-forming part of the tail-clamp PNAs (compare PNA603, PNA649, and PNA648). The T_m was reduced by only 8 °C from the full-length PNA 6-mer triplex to the 4-mer clamp. Furthermore, the thermal stability of tail-clamp PNAs hybridized to the full-length target was not strongly affected by the PNA net charge (compare PNA355$^{(1+)}$, PNA350$^{(2+)}$, PNA602$^{(3+)}$, and PNA603$^{(5+)}$). Finally, substitution of pseudoisocytosine for cytosine (Figure 2a) in the PNA strand engaging in Hoogsteen interactions (compare PNA355 and PNA357) increased T_m by 6 and 8 °C for hybridization to the truncated and full-length target, respectively, as expected from previous results at pH 6.5 where cytosine is only partly protonated (*21*).

Tail-Clamp PNA Binding to Double-Stranded DNA: Effect of a Mixed Sequence Duplex-Forming Extension. To examine the binding to dsDNA by tail-clamp PNAs, PNA was incubated with a ^{32}P-end-labeled DNA restriction fragment containing the complementary target. Helix invasion was monitored by permanganate probing. Permanganate preferentially oxidizes thymines in the displaced DNA strand, which renders the DNA susceptible to alkali cleavage at such reacted positions (*1*, *2*). Alternatively, electrophoretic mobility shift analysis could have been employed for determina-

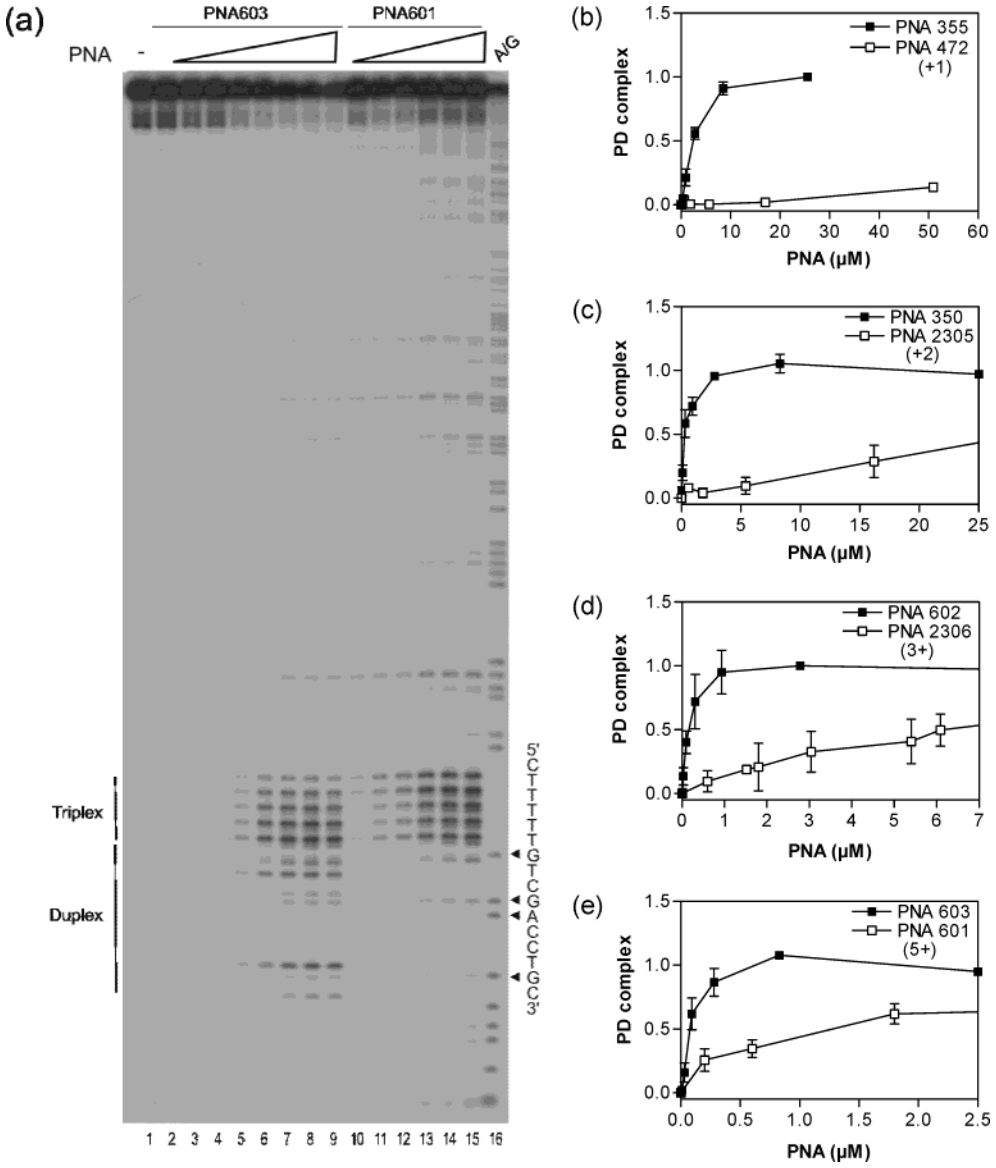

FIGURE 4: Comparison of tail-clamp PNA and homopyrimidine bis-PNA strand invasion as a function of PNA net charge. (a) Autoradiograph showing strand invasion of identically charged tail-clamp PNA (PNA603) and hexamer homopyrimidine bis-PNA (PNA601) as analyzed by permanganate probing as described in Experimental Procedures. The following PNA concentrations were used: without (lane 1), 0.001 μM (lane 2), 0.003 μM (lane 3), 0.01 μM (lane 4), 0.03 μM (lane 5), 0.08 μM (lane 6), 0.3 μM (lane 7), 0.8 μM (lane 8), 2.5 μM (lane 9), 0.2 μM (lane 10), 0.6 μM (lane 11), 1.8 μM (lane 12), 5.4 μM (lane 13), 16 μM (lane 14), and 49 μM (lane 15). The PNA target site is indicated. A/G = sequence marker. (b−e) Results from experiments similar to the one in (a) for the indicated sets of PNAs were quantified by phosphorimaging and displayed as PD complex versus PNA concentration. The signal is taken relative to the plateau for each tail-clamp PNA that is set to 1. The PNA net charge is indicated as are the symbols used.

tions of PNA binding to DNA (*24*). However, this technique was inappropriate because complexes formed with hexameric bis-PNA clamps were not stable during electrophoresis (data not shown).

Because the stability of triplex invasion complexes formed with decameric bis-PNA oligomers is extraordinarily high (*25*, *26*), i.e., the dissociation rate is low ($t_{1/2}$ of several days) and often not measurable, such complexes are usually not at equilibrium in a typical experiment. Thus true thermodynamic equilibrium constants are not practically useful and instead a pseudo-K_d, termed C_{50} and defined as the concentration of PNA that gives 50% strand invasion under a given set of application-relevant experimental conditions, is reported (Table 1). However, for the short-clamp PNAs equilibrium is indeed reached because of fast off-rates (vide infra).

We first asked whether the duplex-forming tail of a simple tail-clamp PNA (PNA355) would invade the DNA duplex target. The results clearly demonstrate that both the triplex domain and the duplex domain do indeed bind to the double-stranded DNA target forming a large P-loop (Figure 3). Most interestingly, the corresponding PNA without the tail duplex domain (PNA472) was not able to form an invasion complex under these conditions, showing a significant thermodynamic stabilization by the tail. As expected, adding the tail in trans did not promote binding. However, the binding efficiency of PNA355 is relatively low (C_{50} 2.5 μM; Table 1) as compared with the best decameric bis-PNAs that bind with C_{50} values in the low nanomolar range (*27*). It has previously been found for homopyrimidine PNAs that equipping PNA oligomers with positive charges can dramatically increase binding efficacy by enhancing the rate of binding (*25*, *28*,

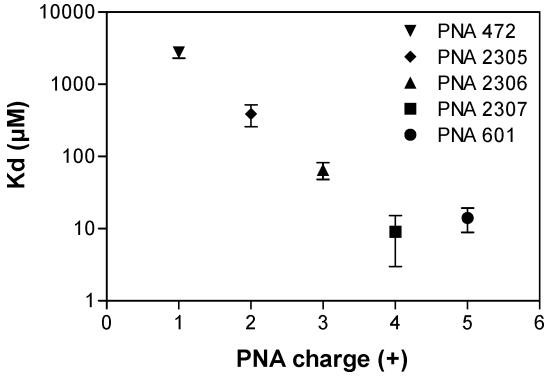

FIGURE 5: DNA affinity of hexameric bis-PNAs as a function of PNA net charge. The dissociation constants for triplex invasion by the relevant hexamer homopyrimidine bis-PNAs were measured by permanganate probing as described in Experimental Procedures and displayed as a function of PNA net charge: PNA472 (1+), PNA2305 (2+), PNA2306 (3+), PNA2307 (4+), and PNA601 (5+).

29). We therefore decided to study tail-clamp PNAs having varying charges in the form of lysine residues and/or a charged amine function in the linker (Figure 4, Table 1). Doubling the charge to 2+ (PNA350) resulted in an ~10-fold decrease in C_{50} (pseudo-K_d); the most direct comparison is with PNA357, which does not contain the J base. Further charge increase to 3+ (PNA602) and 5+ (PNA603) each contributed an additional 2-fold binding increase.

We also prepared the corresponding "tailless" PNA clamps for comparison (PNA2305, PNA2306, PNA2307, and PNA601). The tail-clamp PNAs consistently bound more efficiently to the dsDNA target (lower C_{50}) as compared with the bis-PNA clamps (Figure 4b−e). However, the effect of added charges to the latter was significantly more pronounced. For example, a several hundredfold decrease in C_{50} (K_d) was observed when going from 1+ to 4+ charges (PNA472, PNA2305, PNA2306, and PNA2307; Table 1, Figure 5); increasing the net charge to 5+ (PNA601) did

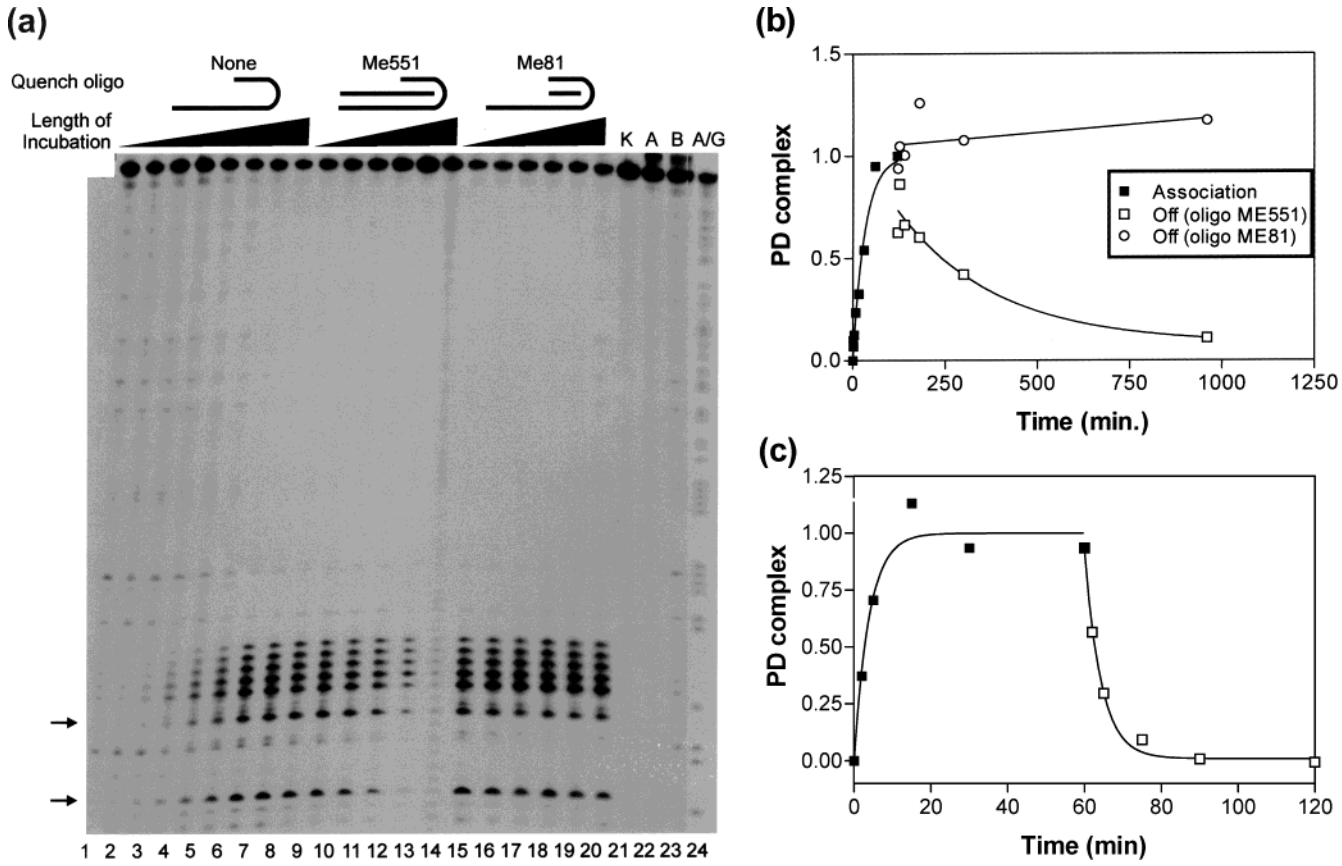

FIGURE 6: Strand invasion kinetics of PNA603 and PNA601. (a) Autoradiograph showing the association and dissociation of tail-clamp PNA603 to its sequence target as determined by permanganate probing. A mastermix containing PNA603 (0.8 μM final concentration) was incubated with the ^{32}P-labeled DNA fragment containing the cognate target at 37 °C. At the desired length of incubation an aliquot was removed and probed with permanganate. At 2 h incubation a molar surplus of quench oligonucleotide (1.7 μM final concentration) complementary to the entire tail-clamp PNA (oligo Me551) or to the hexameric clamp domain only (oligo Me81) was added, and dissociation was followed over time. Association: 1 min (lane 1), 2 min (lane 2), 4 min (lane 3), 8 min (lane 4), 16 min (lane 5), 30 min (lane 6), 1 h (lane 7), and 2 h (lane 8). Dissociation measured in the presence of quench oligo Me551: 2 min (lane 9), 6 min (lane 10), 20 min (lane 11), 1 h (lane 12), 3 h (lane 13), and 16 h (lane 14). Dissociation measured in the presence of quench oligo Me81: 2 min (lane 15), 6 min (lane 16), 20 min (lane 17), 1 h (lane 18), 3 h (lane 19), and 16 h (lane 20). Control without PNA (lane 21, K). Control reactions with oligonucleotides Me551 and Me81 added before PNA (lanes 22 and 23, labeled A and B). A/G sequence reaction (lane 24). (b) Quantification of the data from the experiment shown in (a) depicted as PD complex versus time. The derived first-order association rate constant is 6×10^2 M^{-1} s^{-1} (corresponding to half-binding at 23 min). (c) Data from an experiment similar to the one shown in (a) using bis-PNA601. A mastermix containing PNA601 (1.6 μM) was incubated with the ^{32}P-labeled DNA fragment containing the cognate target at 37 °C. Association (closed squares) was monitored by probing aliquots of the reaction at the desired length of incubation. Then a 2-fold molar surplus of quench oligonucleotide was added, and dissociation was monitored over time (open squares). The derived association and dissociation rate constants are 2×10^3 M^{-1} s^{-1} (corresponding to half-binding in 3 min) and 4×10^{-3} s^{-1} (corresponding to half-dissociation in 3 min), respectively. This yields an equilibrium constant of 2×10^{-6} M, in close agreement with the data presented in Table 1. Arrows indicate diagnostic thymidine residues in the duplex tail target.

not further enhance dsDNA binding efficiency. As these homopyrimidine bis-PNA clamps exhibit comparable thermal stability when binding to a single-stranded target (Table 1), we ascribe this enhancement primarily to an increase in binding on-rate as found for decameric bis-PNAs (*30*). Consequently, the benefit of the tail in terms of relative binding efficiency is significantly decreased with increasing PNA charge.

To better understand this behavior as well as the mechanism of binding, we investigated the kinetics of dsDNA recognition by the best performing PNA pair (PNA603 and PNA601). Tail-clamp PNA603 and bis-PNA601 bound the target with derived on-rates of 6×10^2 and 2×10^3 M^{-1} s^{-1}, respectively (Figure 6). Thus, if anything, association of PNA601 with the target is more rapid as compared with PNA603.

To measure dissociation, an oligonucleotide complementary to the PNA was included to quench free PNA. Virtually no dissociation was detected after overnight incubation using PNA603 as compared with 50% dissociation in ~3 min when using PNA601 (dissociation rate constant of 4×10^{-3} s^{-1}). Thus tail-clamp PNAs bind more efficiently to the sequence target, due to a dramatic reduction of the off-rate, although they unexpectedly bind somewhat more slowly. The control reactions (Figure 6, lanes 22 and 23), in which quencher oligonucleotide was added before PNA, established that no PNA association took place after addition of oligonucleotide.

Most interestingly, the tail-clamp PNA603 could be dissociated ($t_{1/2}$ ~ 3 h) from its dsDNA target if the incubation was conducted in the presence of an oligonucleotide that also included the tail (Figure 6a,b). Furthermore, the permanganate probing indicated that the tail dissociated prior to the clamp. These results therefore (not surprisingly) indicate that the tail binding is much more dynamic (shorter $t_{1/2}$) than clamp binding and that the longer oligonucleotide is able to catch the "breathing" tail and thereby actively catalyze the dissociation via a two-step process.

The ability of the tail-clamp PNAs to discriminate against mismatches was examined by using a PNA carrying three mismatches in the distal part of the tail domain (PNA231). Compared to PNA602, this PNA is expected to recognize only six of the ten bases of the tail. As demonstrated by permanganate probing, triplex invasion occurred efficiently, but strand invasion was entirely absent in the distal part of the tail domain target (Figure 7). Also, the binding affinity of the mismatched PNA231 is slightly (4-fold) decreased compared to the fully matched PNA602 (Table 1).

The target specificity of tail-clamp PNA binding was also investigated by introducing a single G → C substitution in the DNA region that binds the PNA tail domain close to the homopyrimidne junction. The single base alteration abolished binding of the PNA603 tail to the target as evidenced by the lack of oxidation by permanganate of the distal thymidine residue in the duplex target. However, as expected from the experiment with bis-PNA601 (Figure 4e), triplex invasion by the tail-clamp PNA homopyrimidine domain was still observed (data not shown).

Finally, we examined the size requirement of the triplex domain for efficient helix invasion binding using PNA603 as a starting point. These results (Figure 8, Table 1) clearly demonstrate that four bases are too short, while five appear to be sufficient.

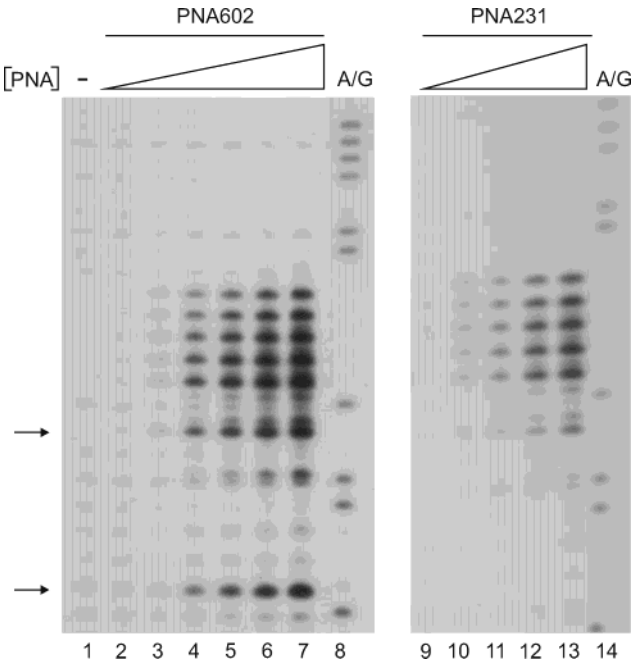

FIGURE 7: Specificity of the tail-clamp PNA duplex-forming extension. Autoradiograph showing strand invasion by identically charged PNAs containing a fully matched (PNA602) or mismatched duplex forming extension (PNA231). The following PNA concentrations were used: without (lane 1), 0.01 μM (lane 2), 0.03 μM (lanes 3 and 9), 0.09 μM (lanes 4 and 10), 0.3 μM (lanes 5 and 11), 0.8 μM (lanes 6 and 12), and 2.5 μM (lanes 7 and 13). A/G = sequence marker. Arrows indicate diagnostic thymidine residues in the duplex tail target.

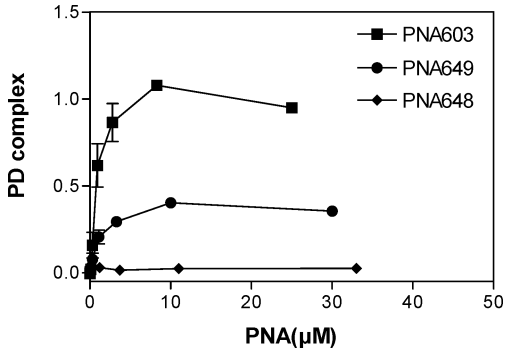

FIGURE 8: Minimal bis-PNA clamp length required for strand invasion. Triplex invasion by identically charged deletion tail-clamp PNAs displayed as PD complex as a function of PNA concentration. Length of clamp domain: PNA603 (6-mer), PNA649 (5-mer), and PNA648 (4-mer). At this point we do not know why some PNAs such as pentadecameric PNA649 saturate the target with only half the permanganate probing signal as compared with hexadecameric PNA603. Whether this for example represents alternate structures will require additional investigation. The signal plateau for PNA603 was set to 1, and the other PNAs were taken relative to this value.

DISCUSSION

The present results show that it is possible to construct tail-clamp PNAs having a very short homopyrimidine triplex clamp domain (five to six nucleobases) and a duplex-forming mixed sequence tail domain in which both domains invade the target helix and in which the tail domain contributes significant binding energy by decreasing dramatically the dissociation rate of the complex. The tail-clamp PNA concept may be exploited for extending the sequence target repertoire of helix-invading PNAs by using short clamps as demonstrated here. Moreover, the duplex-forming tail domains can

specifically extend the P-loop formed. The present results clearly validate the tail-clamp concept but also show that an optimized design is necessary to exploit the effect of the tail. However, the results also indicate that the sequence discrimination power of the tail is limited although more studies are warranted to elucidate the details on binding discrimination and kinetics.

The results also emphasize the advantage of using cationic PNAs to obtain increased on-rate of the dsDNA binding (*25*, *28*, *29*). However, it is striking that the effect of charge is less pronounced for the tail-clamp PNAs (355, 350, 602, and 603) than for the pure PNA clamps (472, 2305, 2306, 2307, and 601). The reason for this is not clear at present, but we note that the tail-clamp PNA603 binds significantly more slowly than the corresponding pure clamp PNA601. Thus the tail appears to interfere to a certain extent with helix invasion, and the mechanism of binding is more complex for tail clamps than for pure clamp PNAs.

On the basis of the strand invasion binding mode reported here many of the applications already described for conventional P-loop-forming homopyrimidine PNAs are likely to have expanded applicability with tail-clamp PNAs. For example, strand invasion complexes formed with tail-clamp PNAs may direct sequence-selective activity of other molecules including S1 nuclease (*31*) and RNA polymerase (*14*) or be used for blockage of transcription elongation as explored in the accompanying paper by Kaihatsu et al. (*35*). Moreover, oligonucleotides complementary to the displaced DNA strand (*5*, *15*) may further stabilize tail-clamp PNA invasion complexes. Tail-clamp PNAs could also be used for placing probes and effector ligands (e.g., fluorophores, EDTA, or psoralen) of interest at a distance from a triplex invasion target. Finally, the tail-clamp PNA binding mode may prove to be useful for exploiting the cooperative binding of a second "effector" PNA in its proximal vicinity (*32*) and for exploration of the PD-loop concept (*5*) used in earring complexes (*33*) and rolling circle amplification (*34*).

ACKNOWLEDGMENT

The excellent technical assistance of Ms. Karin Frederiksen and Ms. Annette W. Jørgensen is greatly acknowledged.

REFERENCES

1. Nielsen, P. E., Egholm, M., Berg, R. H., and Buchardt, O. (1991) Sequence selective recognition of DNA by strand displacement with a thymine-substituted polyamide, *Science 254*, 1497−1500.
2. Nielsen, P. E., Egholm, M., and Buchardt, O. (1994) Evidence for $(PNA)_2$/DNA triplex structure upon binding of PNA to dsDNA by strand displacement, *J. Mol. Recognit. 7*, 165−170.
3. Cherny, D. Y., Belotserkovskii, B. P., Frank-Kamenetskii, M. D., Egholm, M., Buchardt, O., Berg, R. H., and Nielsen, P. E. (1993) DNA unwinding upon strand-displacement binding of thymine-substituted polyamide to double stranded DNA, *Proc. Natl. Acad. Sci. U.S.A. 90*, 1667−1670.
4. Kuhn, H., Demidov, V. V., Nielsen, P. E., and Frank-Kamenetskii, M. D. (1999) An experimental study of mechanism and specificity of peptide nucleic acid (PNA) binding to duplex DNA, *J. Mol. Biol. 286*, 1337−1345.
5. Bukanov, N. O., Demidov, V. V., Nielsen, P. E., and Frank-Kamenetskii, M. D. (1998) PD-loop: a complex of duplex DNA with an oligonucleotide, *Proc. Natl. Acad. Sci. U.S.A. 95*, 5516−5520.
6. Lohse, J., Dahl, O., and Nielsen, P. E. (1999) Double duplex invasion by peptide nucleic acid: a general principle for sequence specific targeting of double stranded DNA, *Proc. Natl. Acad. Sci. U.S.A. 96*, 11804−11808.
7. Izvolsky, K. I., Demidov, V. V., Nielsen, P. E., and Frank-Kamenetskii, M. D. (2000) Sequence-specific protection of duplex DNA against restriction and methylation enzymes by pseudocomplementary PNAs, *Biochemistry 39*, 10908−10913.
8. Demidov, V. V., Protozanova, E., Izvolsky, K. I., Price, C., Nielsen, P. E., and Frank-Kamenetskii, M. D. (2002) Kinetics and mechanism of the DNA double helix invasion by pseudocomplementary peptide nucleic acids, *Proc. Natl. Acad. Sci. U.S.A. 99*, 5953−5958.
9. Nielsen, P. E., and Christensen, L. (1996) Strand displacement binding of a duplex forming homopurine PNA to a homopyrimidine duplex DNA target, *J. Am. Chem. Soc. 118*, 2287−2288.
10. Zhang, X., Ishihara, T., and Corey, D. R. (2000) Strand invasion by mixed base PNAs and a PNA-peptide chimera, *Nucleic Acids Res. 28*, 3332−3338.
11. Hanvey, J. C., Peffer, N. C., Bisi, J. E., Thomson, S. A., Cadilla, R., Josey, J. A., Ricca, D. J., Hassman, C. F., Bonham, M. A., Au, K. G., Carter, S. G., Bruckenstein, D. A., Boyd, A. L., Noble, S. A., and Babiss, L. E. (1992) Antisense and antigene properties of peptide nucleic acids, *Science 258*, 1481−1485.
12. Nielsen, P. E., Egholm, M., and Buchardt, O. (1994) Sequence-specific transcription arrest by peptide nucleic acid bound to the template strand, *Gene 149*, 139−145.
13. Wang, G., Xu, X., Pace, B., Dean, D. A., Glazer, P. M., Chan, P., Goodman, S. R., and Shokolenko, I. (1999) Peptide nucleic acid (PNA) binding-mediated induction of human gamma-globin gene expression, *Nucleic Acids Res. 27*, 2806−2813.
14. Møllegaard, N. E., Buchardt, O., Egholm, M., and Nielsen, P. E. (1994) PNA-DNA Strand displacement loops as artificial transcription promoters, *Proc. Natl. Acad. Sci. U.S.A. 91*, 3892−3895.
15. Broude, N. E., Demidov, V. V., Kuhn, H., Gorenstein, J., Pulyaeva, H., Volkovitsky, P., Drukier, A. K., and Frank-Kamenetskii, M. D. (1999). PNA openers as a tool for direct quantification of specific targets in duplex DNA, *J. Biomol. Struct. Dyn. 17*, 237−244.
16. Demidov, V. V., Broude, N. E., Lavrentieva-Smolina, I. V., Kuhn, H., and Frank-Kamenetskii, M. D. (2001) An artificial primosome: design, function, and applications, *ChemBioChem 2*, 133−139.
17. Demidov, V. V., Kuhn, H., Lavrentieva-Smolina, I. V., and Frank-Kamenetskii, M. D. (2001) Peptide nucleic acid-assisted topological labeling of duplex DNA, *Methods 23*, 123−131.
18. Williams, K. A., Veenhuizen, P. T., de la Torre, B. G., Eritja, R., and Dekker, C. (2002) Nanotechnology: Carbon nanotubes with DNA recognition, *Nature 42*, 761.
19. Bentin, T., and Nielsen, P. E. (2002) In vitro transcription of a torsionally constrained template, *Nucleic Acids Res. 30*, 803−809.
20. Christensen, L., Fitzpatrick, R., Gildea, B., Petersen, K. H., Hansen, H. F., Koch, T., Egholm, M., Buchardt, O., Nielsen, P. E., Coull, J., and Berg, R. H. (1995) Solid-phase synthesis of peptide nucleic acids (PNA), *J. Pept. Sci. 3*, 175−183.
21. Egholm, M., Christensen, L., Dueholm, K., Buchardt, O., Coull, J., and Nielsen, P. E. (1995) Efficient pH independent sequence specific DNA binding by pseudoisocytosine-containing bis-PNA, *Nucleic Acids Res. 23*, 217−222.
22. Sambrook and Russel (2001) *Molecular Cloning, A laboratory manual*, 3rd ed., Cold Spring Harbor Laboratory Press, Cold Spring Harbor, NY.
23. Egholm, M., Buchardt, O., Christensen, L., Behrens, C., Freier, S. M., Driver, D. A., Berg, R. H., Kim, S. K., Nordén, B., and Nielsen, P. E. (1993) PNA hybridizes to complementary oligonucleotides obeying the Watson−Crick hydrogen bonding rules, *Nature 365*, 556−568.
24. Bentin, T., Larsen, H. J., and Nielsen, P. E. (2003) in *Peptide Nucleic Acids. Protocols and Applications* (Nielsen, Ed.) Horizon Scientific Press, Norfolk, England (in press).
25. Griffith, M. C., Riesen, L. M., Greig, M. J., Lesnik, E. A., Sprankle, K. G., Griffey, R. H., Kiely, J. S., and Freier, S. M. (1995) Single and bis peptide nucleic acids as triplexing agents: binding and stoichiometry, *J. Am. Chem. Soc. 117*, 831−832.
26. Kosagonov, Y. N., Stetsenko, D. A., Lubyako, E. N., Kvito, N. P., Lazurkin, Y. S., and Nielsen, P. E. (2000) *Biochemistry 39*, 11742−11747.

27. Bentin, T., and Nielsen, P. E. (2003) Superior duplex DNA strand-invasion by acridine conjugated peptide nucleic acids, *J. Am. Chem. Soc. 125*, 6378−6379.
28. Kuhn, H., Demidov, V. V., Frank-Kamenetskii, M. D., and Nielsen, P. E. (1998) Kinetic sequence discrimination of cationic bis-PNAs upon targeting of double-stranded DNA, *Nucleic Acids Res. 26*, 582−587.
29. Bentin, T., and Nielsen, P. E. (1996) Enhanced peptide nucleic acid binding to supercoiled DNA: possible implications for DNA "breathing" dynamics, *Biochemistry 35*, 8863−8869.
30. Demidov, V. V., Yavnilovich, M. V., Belotserkovskii, B. P., Frank-Kamenetskii, M. D., and Nielsen, P. E. (1995) Kinetics and mechanism of PNA binding to duplex DNA, *Proc. Natl. Acad. Sci. U.S.A. 92*, 2637−2641.
31. Demidov, V., Frank-Kamenetskii, M. D., Egholm, M., Buchardt, O., and Nielsen, P. E. (1993) Sequence selective double strand DNA cleavage by PNA targeting using nuclease S1, *Nucleic Acids Res. 21*, 2103−2107.
32. Kurakin, A., Larsen, H. J., and Nielsen, P. E. (1998) Cooperative strand displacement by peptide nucleic acid (PNA), *Chem. Biol. 5*, 81−89.
33. Kuhn, H., Demidov, V. V., and Frank-Kamenetskii, M. D. (1999) Topological links between duplex DNA and a circular DNA single strand, *Angew. Chem., Int. Ed. 38*, 1446−1449.
34. Kuhn, H., Demidov, V. V., and Frank-Kamenetskii, M. D. (2002) Rolling-circle amplification under topological constraints, *Nucleic Acids Res. 30*, 574−580.
35. Kaihatsu, K., Shah, R. H., Zhao, X., and Corey, D. R. (2003) *Biochemistry 42*, 13996−14003.

BI0351918